# Fatigue Analysis of the Piston Rod in a Kaplan Turbine Based on Crack Propagation under Unsteady Hydraulic Loads

**X Liu**[1], **Y Y Luo**[1], **Z W Wang**[1]
[1]State Key Laboratory of Hydroscience and Engineering & Department of Thermal Engineering, Tsinghua University, Beijing 100084, PR China

E-mail: wzw@mail.tsinghua.edu.cn

**Abstract.** As an important component of the blade-control system in Kaplan turbines, piston rods are subjected to fluctuating forces transferred by the turbines blades from hydraulic pressure oscillations. Damage due to unsteady hydraulic loads might generate unexpected down time and high repair cost. In one running hydropower plant, the fracture failure of the piston rod was found twice at the same location. With the transient dynamic analysis, the retainer ring structure of the piston rod existed a relative high stress concentration. This predicted position of the stress concentration agreed well with the actual fracture position in the plant. However, the local strain approach was not able to explain why this position broke frequently. Since traditional structural fatigue analyses use a local stress strain approach to assess structural integrity, do not consider the effect of flaws which can significantly degrade structural life. Using linear elastic fracture mechanism (LEFM) approaches that include the effect of flaws is becoming common practice in many industries. In this research, a case involving a small semi-ellipse crack was taken into account at the stress concentration area, crack growth progress was calculated by FEM. The relationship between crack length and remaining life was obtained. The crack propagation path approximately agreed with the actual fracture section. The results showed that presence of the crack had significantly changed the local stress and strain distributions of the piston rod compared with non-flaw assumption.

## 1. Introduction

Hydropower has become a proven, extremely flexible, and well-advanced technology for more than one century. Although current hydropower technology is very mature, there is still some room for further improvement. Interactions of turbine components generally occur frequently, sometimes even are quite severe. Except for common pressure fluctuations with high or low frequency, there still are many complex or unclear factors to cause acute interactions. For example, when a turbine is running at an off-design condition, there would be serious vibration due to pressure fluctuations. For a majority of hydropower plants, turbines have operated for decades, and in many of them the current operating conditions have changed from the original design specified. These kind of differences may cause vibrations and some have presented cracks in parts of components of turbines produced by fatigue [1-3]. Within all hydropower applications, there will always be flaws in structures, but to different degrees. Cyclic loading can cause flaws to develop into cracks, or make the existing crack continuously grow by fatigue progress. Even when the load is lower than the design load, the formation and propagation of cracks may lead the failure or damage of the key components of the turbine. Existing flaws and potential resulting risk will limit the operating time of the unit. Some plants have to be compelled to shut down for one month and possibly longer to repair these fatigue damage, which has resulted in enormous

economic losses. Therefore, fatigue problems must be solved or effectively prevented to ensure the units run safely and steadily within their design life.

In most cases, the fatigue cracks are presents in regions that have a metallurgical or structural discontinuity and are subjected to higher stresses. Local stress and strain approaches have been adopted to estimate the fracture life of a structure subjected to fatigue loads[4]. However, fatigue involves a very complex interaction of different metallurgical, mechanical and technological factors and is still only partly understood[5]. These factors include: type frequency and amplitude of load, material model, member size, material flows, manufacturing method, operating temperature, environmental operating conditions etc.[6]. Stress-life and strain-life methods focus on the stress and strain state of the structure, highly depending on the empirical parameters selections, which inevitably lead to poorly reliable estimation. A damage tolerance approach based on linear elastic fracture mechanics (LEFM) describes crack behaviour using concepts from both applied mechanics and material science by combing the effect of stress state and flaws. Nevertheless it's not common to see related papers to calculate the crack propagation in hydraulic turbines by means of LEFM. The aforementioned concepts applied herein, and the specific research object is a piston rod of a Kaplan turbine installed in one hydropower plant in China.

## 2. Fatigue life prediction approaches

### *2.1 Local strain approach*

The classical Coffin-Manson-Basquin formula[7] defines the relationship between strain amplitude $\varepsilon_a$ and the number of cycles to failure $N_\mathrm{f}$:

$$\Delta\varepsilon_\mathrm{t} = \Delta\varepsilon_\mathrm{e} + \Delta\varepsilon_\mathrm{p} = \frac{\sigma_\mathrm{f}'}{E}(2N_\mathrm{f})^\mathrm{b} + \varepsilon_\mathrm{f}'(2N_\mathrm{f})^\mathrm{c} \tag{1}$$

where the total strain amplitude $\Delta\varepsilon_\mathrm{t}$ is divided into elastic $\Delta\varepsilon_\mathrm{e}$ and plastic $\Delta\varepsilon_\mathrm{p}$ components. $2N_\mathrm{f}$ is the number of cycles to fatigue failure. b and c are the fatigue strength exponent and fatigue ductility exponent respectively. This formula is more adequate to model low cycle fatigue[8], since it relates the plastic strain amplitude $\Delta\varepsilon_\mathrm{p}$, with the number of reversals to failure, $2N_\mathrm{f}$.

If the Morrow mean stress correction is to be applied, the mean stress for each cycle is calculated by:

$$\sigma_\mathrm{m} = \frac{\sigma_\mathrm{max} + \sigma_\mathrm{min}}{2} \tag{2}$$

And Equation (1) becomes:

$$\Delta\varepsilon_\mathrm{t} = \frac{(\sigma_\mathrm{f}' - \sigma_\mathrm{m})}{E}(2N_\mathrm{f})^\mathrm{b} + \varepsilon_\mathrm{f}'(2N_\mathrm{f})^\mathrm{c} \tag{3}$$

For a stable hysteresis curve, it is suggested[9] that it can be described by a cycle of deformation being the sum of the elastically and plastically ranges, so:

$$\Delta\varepsilon = \frac{\Delta\sigma}{E} + 2\left(\frac{\Delta\sigma}{2K'}\right)^{\frac{1}{n'}} \tag{4}$$

where, $n'$ is cyclic hardening exponent, and $K'$ is cyclic strength coefficient.

### *2.2 Fracture mechanics approach*

The crack growth life calculation method is developed upon LEFM. A stress intensity factor (SIF) can be expressed by nominal load $\sigma_{ij}(r,\theta)$ and a crack length $a$, in polar coordinates $(r,\theta)$ with origin at the crack tip:

$$K = \sigma_{ij}(r,\theta)\cdot\sqrt{\pi\cdot a}\,/f_{ij}(\theta)[\mathrm{MPa}\cdot\mathrm{mm}^{0.5}] \tag{5}$$

SIF is a fundamental parameter of crack growth analysis, and depends on sample geometry, the size and location of the crack, and the magnitude and the modal distribution of loads on the material. $f_{ij}(\theta)$ is a dimensionless quantity that varies with the load and geometry.

For most cases in practice, the crack is cyclically loaded in a way such that at the crack front non-proportional mixed-mode situations will occur. Since these fatigue load conditions are a combination of various load sequences originated from different sources[10]. Here, a mixed mode stress intensity factor $\Delta K_{\mathrm{MM}}$ range was introduced replacing the conventional $\Delta K$ in Paris crack growth rate equation:

$$\frac{\mathrm{d}a}{\mathrm{d}N} = \mathrm{C}(\Delta K_{\mathrm{MM}})^{\mathrm{m}} \tag{6}$$

where, $a$ is the crack length, $\Delta K_{\mathrm{MM}}$ is mixed mode stress intensity factor range, C and m are the material constants. $\Delta K_{\mathrm{MM}}$ can be obtained by the *M*-integral.

The relationship between the *M*-integral and the stress intensity factors as

$$\begin{aligned} M = -\frac{1}{2}\Big[ & K_I^{(1)}\mathrm{Im}\left(m_{2i}N_{ij}^{-1}K_j^{(2)}\right) + K_I^{(2)}\mathrm{Im}\left(m_{2i}N_{ij}^{-1}K_j^{(1)}\right) + K_{II}^{(1)}\mathrm{Im}\left(m_{1i}N_{ij}^{-1}K_j^{(2)}\right) \\ & + K_{II}^{(2)}\mathrm{Im}\left(m_{1i}N_{ij}^{-1}K_j^{(1)}\right) + K_{III}^{(1)}\mathrm{Im}\left(m_{3i}N_{ij}^{-1}K_j^{(2)}\right) \\ & + K_{III}^{(2)}\mathrm{Im}\left(m_{3i}N_{ij}^{-1}K_j^{(1)}\right)\Big] \end{aligned} \tag{7}$$

where Im is the imaginary component of the bracketed quantities with a summation being applied to repeated indices. The parameter $m_{ij}$ and matrix $N_{ij}$ describe the near-tip behaviour of a crack.

The *M*-integral has been used with the extended finite element method (X-FEM) by Dolbow and Gosz[11], and with the element-free Galerkin (EFG) method by Rao and Rahman[12]. Among these techniques, the finite element method (FEM) is one of the most popular methods. In the context of finite elements, the evaluation of area and volume integrals lead to more accurate and stable results than direct integration along a contour[13]. More details were discussed by Kim and Paulino[14] and by Wawrzynek and Carter[13].

## 3. Case study

### *3.1 Background introduction*

A Kaplan turbine unit was put into operation in 1995. On February 2000, this unit was firstly found to be vibrating severely. The oil level in the oil collection groove then rapidly dropped. Examination revealed the central axis of the piston rod had broken at the joint of the nut with the crosshead, the broken part had fallen into the cone (Figure 1. a)[15]. So the plant changed the nut structure to a retainer ring structure. The structural strength of the new design had passed. However, 5 years later, the retainer ring structure also broke at the same location (Figure 1. b). A comprehensive investigation was then performed and showed that the broken location was confirmed existing stress concentration but not fully explained the fracture reason.

a) Nut structure b) Retainer ring structure

**Figure 1.** Schematic of fractured piston rods.

For some key components of a turbine like blades and the piston rod, unsteady hydraulic loads are the main factor to induce their fatigue fracture. In some off-design operating zones, hydraulic pressure

fluctuates severely. And this strong unsteady load finally was transferred to the piston rod by the blade-control system, causing the stress and strain rate to very sharply.

*3.2 Transient dynamic analysis*

Since the piston rod was located inside of the runner body and contacted with other parts, it's difficult to clearly describe the load transfer relation. Based on the unsteady flow simulation of 3D full flow model, this research analysed dynamic stresses of the crosshead-piston rod system by means of nonlinear contact technology.

The calculations were performed for two typical operating conditions. GK1 is small blade angle and guide vane opening, while GK3 is large blade angle and guide vane opening near the optimum operating point. The operating parameters of the two selected conditions are list in Table 1.

**Table 1.** Operating parameters for small, medium and large blade angles.

| Operating condition | Head (m) | Power (MW) | Guide vane opening (%) | Blade angle (°) |
|---|---|---|---|---|
| GK1 | 58.5 | 100 | 37.3 | 6.6 |
| GK3 | 58.5 | 210 | 64.0 | 18.0 |

Each blade torque was obtained by 3D unsteady simulation. The computed torques for two typical blade angles are shown in Figure 2.

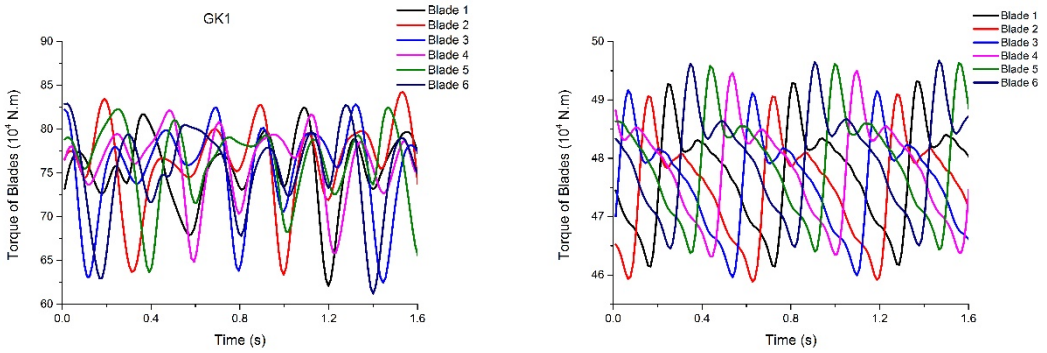


a) GK1 b) GK3

**Figure 2.** Torques on all six blades for GK1 and GK3.

For condition GK3, the torques on the blade pivot fluctuated with the runner rotation frequency, with a 60° phase angle on adjacent blades. And for condition GK1, the blade torque fluctions were accompanied by increased turbulence with a 120° phase angle on adjacent blades. Figure 2 also shows that the mean values and amplitudes of the torques were smaller for condition GK3 near the optimum operating point than those in small blade angle for condition GK1. According to the power station's operating records, the operating oil pressure inside the piston chamber was normal when the turbine was running near GK3, but the oil pressure inside the chamber was extremely high when it was operating near GK1.

The finite element model of a multi-body system was developed as shown in Figure 3. The piston rod, retainer ring, crosshead and key were connected through contact configuration. The whole system was subjected to gravity and centrifugal acceleration due to the rotational motion. Forces acting on the crosshead were transferred from six blade torques which was introduced in reference[15]. The end time of transient analysis was three periods. Through the multi-body system simulation, the accurate stress strain distribution could be obtained in conditions GK1 and GK3. The computation results would provide a reliable load spectrum to carry out a life prediction. Furthermore, these results could provide valuable information for the security of the plant operation.

where， $F_{czj}$ is the equivalent force acting on the crosshead by the blade. $BA$ is blade angle， $T_b$ is the single blade torque, $L_1$ and is the length of blade lever, is the angle between the blade link and the crosshead.

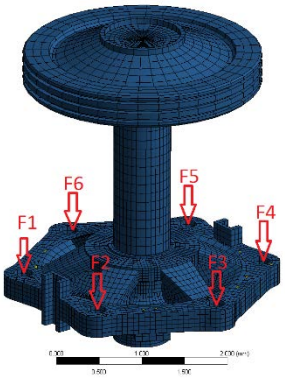


**Figure 3.** FE model and loading distribution of the multibody-system.

The original material of the piston rod was hammered steel 20SiMn. However, due to the lack of the exact material fatigue information, the material selected for analysis here is structural steel BS4360 Grade 43D. The material properties and performance of both are quite similar, as illustrated in Table 2.

**Table 2.** Material properties of Structural Steel BS4360 Grade 43D.

| | **20SiMn** | **BS4360** |
|---|---|---|
| Density | 7850 kg/m$^3$ | 7850 kg/m$^3$ |
| Young's Modulus $E$ | 2.07 GPa | 2.07 GPa |
| Poisson's Ratio | 0.3 | 0.3 |
| Tensile Yield Strength | 275 MPa | 281 MPa |
| Tensile Ultimate Strength | 490 Mpa | 490 MPa |
| Fatigue strength coefficient $\sigma_f'$ | - | 803 Mpa |
| Fatigue ductility coefficient $\varepsilon_f'$ | - | 0.197 |
| Strength Exponent b | - | -0.086 |
| Ductility Exponent c | - | -0.445 |
| Fatigue Cutoff $N_c$ | - | 2e8 |
| Cyclic Strain Hardening Exponent $n'$ | - | 0.191 |
| Cyclic Strength Coefficient $K'$ | - | 983 Mpa |

Dynamic stress time-domain graph of the point of maximum stress for two conditions are shown in Figure 4 and Figure 5, the calculated maximum stress point located at the root of the fillet of the piston rod, contact with the retainer ring. This location agreed well with the actual fracture position for nut and retaining ring structures.

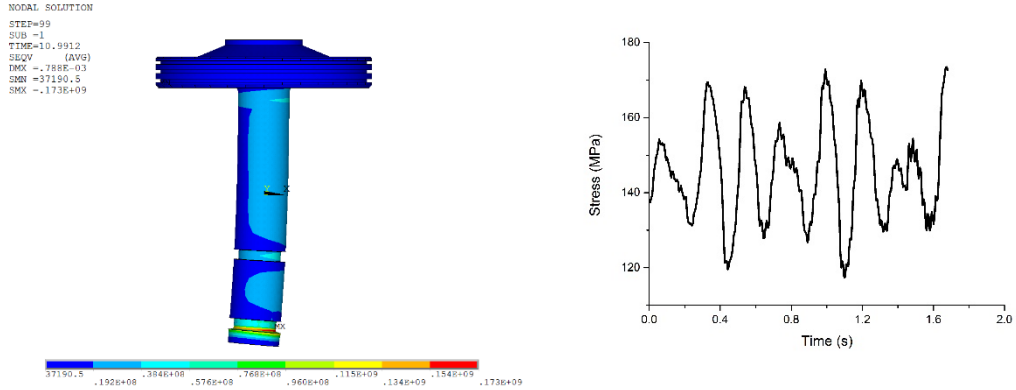


**Figure 4.** Dynamic stress time-domain graph of the point of maximum stress in GK1.

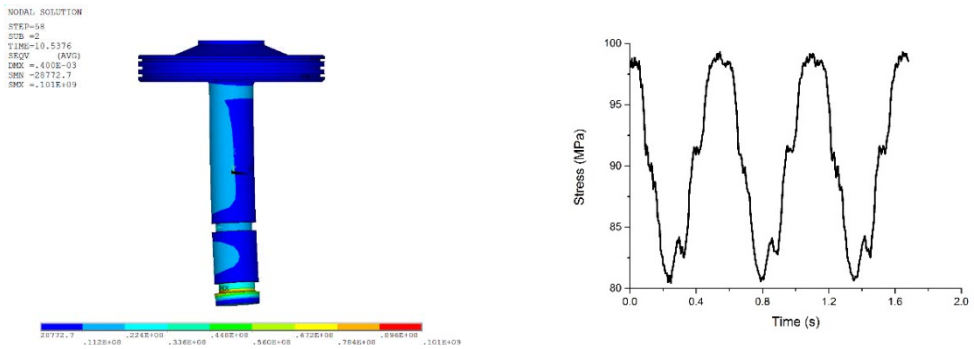


**Figure 5.** Dynamic stress time-domain graph of the Maximum stress point in GK3.

The mean stress at the point of maximum stress for GK1 is 145.2 MPa with a maximum amplitude of 48.2 MPa, and the mean stress at the point of maximum stress for GK3 is 90.4 MPa with an amplitude of 10.0 MPa. It indicated that the stress environment in GK1 were relatively poor, and stresses varied greatly in small blade angle. The stress ratio in GK1 was 33.2%, much higher than in GK3, which resulted in fatigue in the piston rod. Therefore, the high dynamic stresses were the main reason for the fracture of the retainer ring structural piston rod.

### *3.3 Life prediction by local strain approach*

Condition GK1 is the key fatigue operating condition, using the mean dynamic stress $\sigma_{\mathrm{m}}$, amplitude $\Delta\sigma$, according to Equation (4), the strain amplitude could be got:

$$\Delta\varepsilon = \frac{\Delta\sigma}{E} + 2\left(\frac{\Delta\sigma}{2K'}\right)^{\frac{1}{n'}} = \frac{57.4}{207000} + 2\times\left(\frac{57.4}{2\times 983}\right)^{\frac{1}{0.191}} = 0.000277$$

Then, by substituting $\Delta\varepsilon$ into Equation(3):

$$\Delta\varepsilon = \frac{\sigma_{\mathrm{f}}' - \sigma_{\mathrm{m}}}{E}(2N_{\mathrm{f}})^{\mathrm{b}} + \varepsilon_{\mathrm{f}}'(2N_{\mathrm{f}})^{\mathrm{c}} = \frac{803 - 145.2}{207000}\times(2N_{\mathrm{f}})^{-0.086} + 0.197\times(2N_{\mathrm{f}})^{-0.455}$$

The following is obtained:

$$N_{\mathrm{f}} > 10^{9}$$

$N_{\mathrm{f}} > 10^{9}$ implied fracture should not occur even when the piston rod was long-running at the high dynamic stresses of condition GK1. In fact, the strength check of new piton rod design was carried out in 2000. And the retainer ring structure was safe under condition GK1. In this case, the traditional local stress-strain approach was not adequate for such a specific situation. Because this rule is developed by lots of standard test specimens, and is an average relationship of massive test data. These kinds of tests are normally geometric simple and tested under uniaxial loading. For such a complex loading in the piston rod, local stress-strain approach need more correction based on situ data, and the correction is only valid for this case.

### *3.4 Life prediction by crack propagation approach*

The diameter of the piston rod reached 670 mm. It is difficult to guarantee that no flaws exist in the piston rod at such size. But whether or not flaws exist has a significantly impact on structural fatigue life, it will greatly reduce the service time of the structure. Referencing the actual fracture section in Figure 1, a semi-ellipse crack with a depth 2 mm and width 4 mm in a visible size was assumed to locate at the root of the fillet. Actually, this size chosen due to mesh quantity may be a little bit large. In future, the initial crack size will be investigated to explore the effect of the initial crack. The finite element schematic is shown in Figure 6. The material was still structural steel BS4360 grade 43, for which c and m in Paris' Law are equal to $1.834\times10^{-13}$ and 3.0, respectively; for $\Delta a/\Delta N$ in mm/cycle and $\Delta K$ in

$MPa \cdot mm^{0.5}$ [16]. The mesh sensitivity analysis was carried out in Table 3. Consequently, 6 mesh contours and 8 circumferential divisions were chosen in crack propagation analysis.

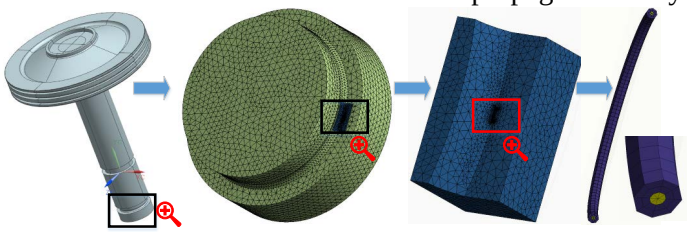

**Figure 6.** The location and mesh schematic of the initial ellipse crack.

**Table 3.** Mesh sensitivity analysis of the crack front at 2 mm.

| Mesh contours | Circumferential Divisions | Median SIF K1 | Median SIF K2 | Median SIF K3 |
|---|---|---|---|---|
| 2 | 8 | 318.54 | 7.4771 | 4.9177 |
| 4 | 8 | 316.19 | 4.5962 | 5.4241 |
| 6* | 8* | 317.13 | 7.8244 | 6.6107 |
| 6 | 16 | 317.13 | 7.8245 | 6.6106 |
| 8 | 8 | 315.96 | 6.6651 | 5.14 |
| 10 | 8 | 311.58 | 4.1087 | 5.3538 |

According to the operating records at the hydropower plant: the operating head was generally greater than 47 m; output power was between 80 MW and 110 MW for 30% of the time; output power was between 110 MW and 140 MW for 15% of the time, and; output power was greater than 140 MW 50% of the time. The average annual operating hours were approximately 4000, and the time period from installation until failure was 6 years. The load spectrum was made according to these operating data with some simplification. GK1 made up 30% of running time, and GK3 made up the remaining 70%. Figure 7 showed the load spectrum and rainfall counting histogram.

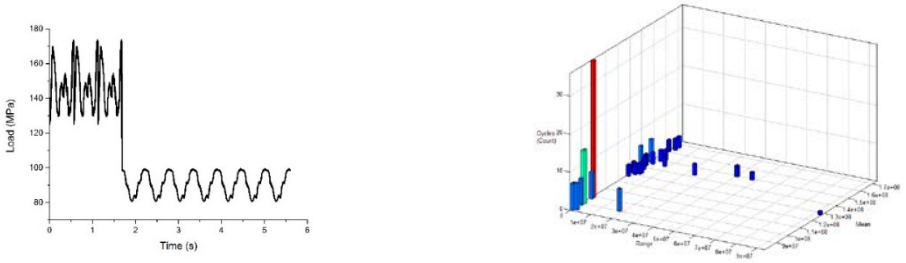


**Figure 7.** Load spectrum and rainfall counting histogram of the critical location.

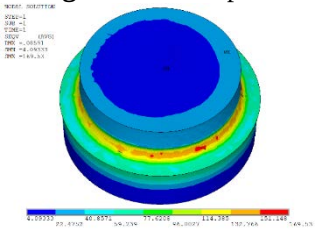

a) σ=169.53. No Crack.

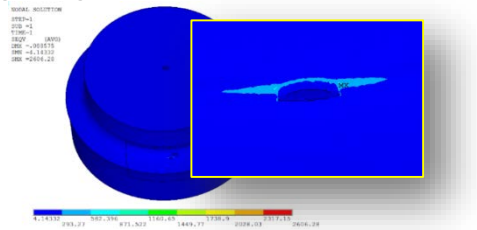

b) σ=2606, SIF=347 , a=5.9

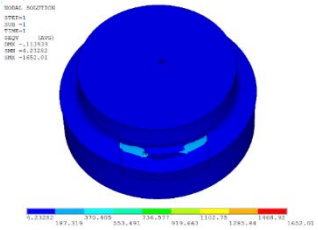

c) σ=1791, SIF=498, a=14

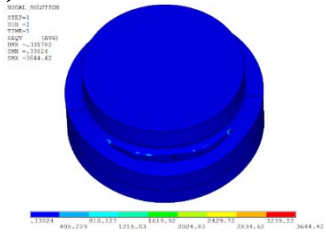

d) σ=3644, SIF=1072, a=217

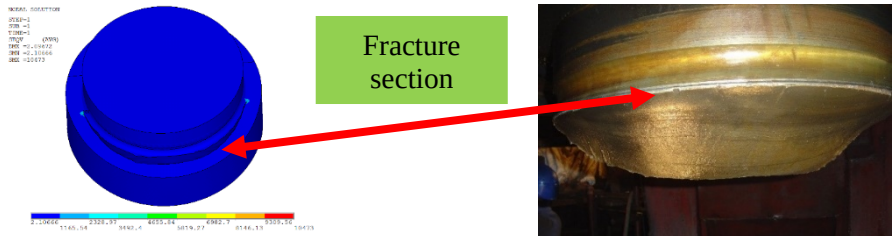


e) σ=10473, SIF=2122, a=357

**Figure 8.** Stress distributions for different crack lengths.

Figure 8 illustrated the stress distributions for different crack lengths, units in MPa, MPa $mm^{0.5}$ and mm. These crack shape were calculated via equations (6) and (7). The whole stress level of no flaws model is within the structural yield strength. After formation of the crack, because of the LEFM assumption, the stress and strain changed is $1/\sqrt{r}$, $r$ is the displacement to the crack tip, $r \ll a$. The stress becomes singular at the crack tip (much more than yield strength). This would be a disaster if the material is fully brittle. In fact, as a results of the ductility, a very small plastic zone around the crack tip will be created. The peak stress then is levelled off. Although relative equations are no longer valid in this plastic area because they are all based on an assumed elastic behaviour. This does not prevent the use of SIFs[17]. Actually, the effective integral radius $r_M$ of the *M*-integral is significantly larger than the size of the plastic zone, but is still chosen small enough to crack length. The stresses in Equation (5) are still working on this integral path. As a consequence, the value of SIFs by the *M*-integral should still give a meaningful indication of the severity of the stresses acting on the crack tip zone. Ultimately, this singular peak stress is symbolic to reflect the size of SIFs. The relationship between crack length, SIFs and maximum stress are plotted in Figure 9.

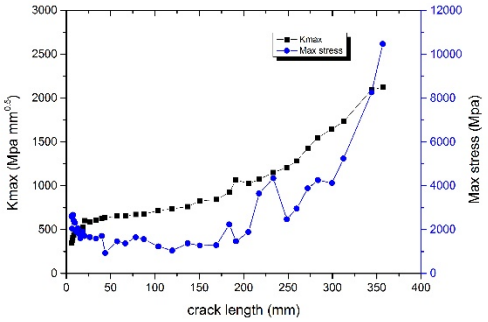


**Figure 9.** Plot of crack length vs SIFs and peak stress (Von Mises).

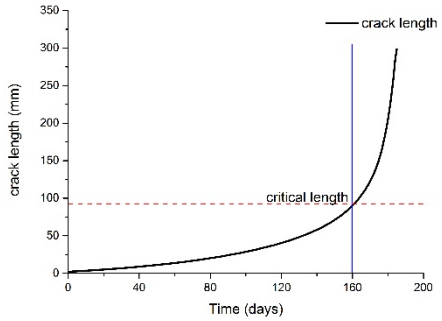


| Crack length | remaining life (days) |
|---|---|
| 2mm | 185 |
| 4mm | 170 |
| 10mm | 138 |
| 20mm | 105 |
| 30mm | 79 |
| 40mm | 65 |
| 50mm | 51 |

**Figure 10.** Plot of cyclic time vs crack length.

**Table 4.** Crack length and left life.

Then, based on Paris Equation (6) and the load spectrum in Figure 7, the relationship between service time and crack length was determined, as shown in Figure 10. Here, the critical crack length was 90 mm defined as 85% of total service time. When the crack length became greater than 90 mm, the crack

growth rate sharply increased and the failure would happen soon. This value is not a constant, but can be determined with the aid of economical and safe factors. Either way, the structure must be repaired or replaced when the crack length approaches to the critical length.

Generally, the percentage of the crack formation and small crack propagation was 60%. It's important to note that this percentage was obtained purely by author's past project experience. The more accurate value should be calculated via crack initiation life analysis. As a case study and methodology discussion, this level of error can be acceptable. The life of the piston rod with an initial 2mm crack is:

$$N_{\text{life}} = \frac{N_{\text{longcrack}}}{\text{Time}_{\text{percent}}(\%)} = \frac{160}{1-60\%} = 400(days)$$

The annual working time is 4000 hours, the 400 days service time of the piston rod corresponds to about 3 years, which is half of the true service time. In additional, this prediction is conservative. There are two probable reasons for this. The first is that the load spectrum was only made up of GK1 and GK3. GK1 is a high stress operating condition and accounted for 30% in load spectrum. However, this percentage should be much lower in reality. Through this case, it also illustrated that an accurate load spectrum had a great influence on crack growth prediction. The second reason for the estimate being conservative is that it is no constant for 60% of the time of crack formation and small crack growth, it would be determined by operating conditions, materials used, residual stresses, crystal structures, and initial flaws. There is lack of enough information to get an accurate percentage in this case.

## 4. Conclusion

The crack growth process within the piston rod was simulated by means of FEM, and a relationship between crack length and remaining life was obtained. The crack began to grow from 2mm, the path (i.e. crack length and propagation direction) was calculated, and the final crack propagation shape was similar with the actual fracture section, shown in Figure 8 e). The critical length was chosen based on a security standpoint, and this value is a valuable information for the plant operators to make a proper maintenance time.

The case also illustrated the limitation of the local strain approach. Generally, the critical damage value $D_{\text{CR}}$ is given one. However, lots of tests have proven this value could be 0.1~10. Even for a simple shell case under a well-defined loading, large differences in predicted fatigue lives were found, ranging from 1.8 to 20.7 years[18]. This uncertainty make the traditional prediction unreliable. Although crack growth prediction can't give an accurate total service life, either. But the remaining life vs crack length which can be only obtained by crack growth prediction approach is reliable and more valuable for the plant operators.

Mixed mode crack growth behaviour is difficult to be evaluated by experimental tests or experimentally inaccessible. Because it needs to test a large number of materials and structural components in a very short time. This implies the benefit of using numerical computational methods to estimate the 3D mixed mode crack propagation. The accuracy of the crack propagation estimate obtained by applying methods in this paper are still under thorough investigation. However, the work is a field of scientific interest and to provide a collection of references and a specific case for further research. And it is truly a very useful tool and is believed to become a promising analysis technique in the future.

## Acknowledgments

Special thanks are due to the National Natural Science Foundation of China under Contract (No. 51279083) for supporting the present work.

## Nomenclature

| | | | |
|---|---|---|---|
| $a$ | Crack length | $N_{\text{f}}$ | Half of number of cycles to fatigue failure |
| b | Fatigue strength exponent | $u$ | Displacement vector |
| c | Fatigue ductility exponent | $W$ | Strain energy density |

| | | | |
|---|---|---|---|
| $J$ | *J*-integral | $\theta$ | Kink angle |
| $K$ | Stress intensity factor | $\Delta\varepsilon_{\mathrm{e}}$ | Elastic strain amplitude |
| $K'$ | Cyclic strength coefficient | $\Delta\varepsilon_{\mathrm{p}}$ | Plastic strain amplitude |
| $M$ | *M*-integral | $\Delta\varepsilon_{\mathrm{t}}$ | Total strain amplitude |
| $n'$ | Cyclic hardening exponent | $\sigma$ | Stress |
| $N$ | Number of cyclic loading | | |

## References

[1] Flores M 2012 A fatigue analysis of a hydraulic Francis turbine runner *World J. of Mechanics* **02** 28-34
[2] Xiao R F, Wei C X, Han F Q, and Zhang S Q 2001 Study on dynamic analysis of the Francis turbine runner *Large Electric Machine and Hydraulic Turbine* **7** 41-3
[3] Rao J, Nimbekar P, Misra R, and Singh A 1998 Application of local stress-strain approach to predict fracture initiation of a Francis turbine runner blade *7th Int. Symp. on Transport Phenomena and Dynamics of Rotating Machinery* (Hawaii, USA) 22-6
[4] Tanaka H 1990 Vibration behaviour and dynamic stress of runners of very high head reversible pump-turbines *15th IAHR Symp.* (Belgrade, Serbia)
[5] Stephens R I and Fuchs H O 2001 *Metal fatigue in engineering* (Wiley New York)
[6] Salam I, Abid M, and Malik M A 2007 Crack growth prediction in a thick cylinder under fatigue loading-an FEA *Int. J. of Systems Applications, Engineering & Development* **3** 51-5
[7] Morrow J 1965 Cyclic plastic strain energy and fatigue of metals *ASTM STP* **378** 7
[8] Jesus A M P d, Silva A L L d, Figueiredo M V, Correia J A F O, Ribeiro A S, and Fernandes A A 2011 Strain-life and crack propagation fatigue data from several Portuguese old metallic riveted bridges *Engineering Failure Analysis* **18** 148-63
[9] Martin J, SINCLAIR G, and TOPPER T 1971 Computer based simulation of cyclic stress- strain behavior with applications to fatigue *Materials Research and Standards* **11** 23-8
[10] Zerres P and Vormwald M 2014 Review of fatigue crack growth under non-proportional mixed-mode loading *Int. J. of Fatigue* **58** 75-83
[11] Dolbow J and Gosz M 2002 On the computation of mixed-mode stress intensity factors in functionally graded materials *Int. J. of Solids and Structures* **39** 2557-74
[12] Rao B and Rahman S 2003 Mesh-free analysis of cracks in isotropic functionally graded materials *Engineering Fracture Mechanics* **70** 1-27
[13] Wawrzynek P, Carter B, and Banks-Sills L 2005 *The M-integral for computing stress intensity factors in generally anisotropic materials* (National Aeronautics and Space Administration, Marshall Space Flight Center)
[14] Kim J H and Paulino G H 2003 An accurate scheme for mixed‐mode fracture analysis of functionally graded materials using the interaction integral and micromechanics models *Int. J. for Numerical Methods in Engineering* **58** 1457-97
[15] Wang Z W, Luo Y Y, Zhou L J, Xiao R F, and Peng G J 2008 Computation of dynamic stresses in piston rods caused by unsteady hydraulic loads *Engineering Failure Analysis* **15** 28-37
[16] Xiang Z, Lie S T, Wang B, and Cen Z 2003 A simulation of fatigue crack propagation in a welded t-joint using 3d boundary element method *International Journal of Pressure Vessels and Piping* **80** 111-20
[17] Schijve J 2004 *Fatigue of structures and materials* (Springer Netherlands)
[18] Fricke W, Cui W, Kierkegaard H, Kihl D, Koval M, Mikkola T, Parmentier G, Toyosada M, and Yoon J H 2002 Comparative fatigue strength assessment of a structural detail in a containership using various approaches of classification societies *Marine Structures* **15** 1-13